Scalar waves in a wormhole geometry

Sayan Kar* and Deshdeep Sahdev†
Department of Physics, Indian Institute of Technology, Kanpur 208 016, India

Biplab Bhawal‡
Mehta Research Institute of Mathematics and Mathematical Physics 10, Kasturba Gandhi Marg, Allahabad 211 002, India
(Received 23 July 1993)

The reflection and transmission of massless scalar waves in the curved background geometry of a typical Lorentzian wormhole (in 2+1 and 3+1 dimensions) are discussed. Using the exact solutions which involve modified Mathieu (in 2+1 dimensions) and radial oblate spheroidal (in 3+1 dimensions) functions, explicit analytic expressions are obtained for the reflection and transmission coefficients at specific values of the quantity ωb_0 (ω being the energy of the scalar wave and b_0 the throat radius of the wormhole). It is found that both near-perfect reflection as well as transmission are possible for specific choices of certain parameters.

PACS number(s): 04.20.Cv, 11.10.Qr

I. INTRODUCTION

Ever since Morris and Thorne [1] and Morris, Thorne, and Yurtsever [2] rekindled interest in Lorentzian wormholes there has been a steady flow of papers discussing various questions related to these spacetimes. The possibility of constructing time machines and the requirement of matter violating the weak energy condition (WEC) have been the two major issues on which a fair amount of work has been done. For static geometries, Morris and Thorne had shown that without WEC-violating matter it is impossible to have a wormhole geometry. The fact that there exist quantum states for which the expectation value of the energy-momentum tensor violates all energy conditions [3] led them to conclude that such matter could probably exist in the quantum regime. Other attempts at justifying the existence of such matter include the use of the Casimir effect [4] and squeezed states [5]. Alternative models of gravity have also been explored and the role of WEC violation in connection with wormholes has been investigated in some detail. $R+R^2$ theory in four dimensions yielded the same results as in general relativity (GR) [6]. The nonsymmetric theory of gravity due to Moffat also had nothing new in this context [7]. In higher dimensions ($D>4$), the Einstein-Gauss-Bonnet theory had a certain positive result for negative values of the coupling coefficient of the Gauss-Bonnet term [8].

Apart from the study of the WEC in the context of wormholes, Visser [9] has done some interesting work on the construction of such geometries using "Schwarzschild surgery." The Cauchy problem in spacetimes with closed timelike curves has been discussed in detail for the massless scalar field [10]. Recently Kim [11] has studied "particle creation" due to time travel through a wormhole. On the other front Roman [12] has constructed a solution which is a nonstatic metric with the required energy-momentum tensor violating the WEC. Such a geometry actually evolves in time and might be a way of actually producing wormholes. Hochberg and Kephart [13] have discussed the possible resolution of the "horizon problem" by constructing a hypothetical "wormhole cosmology" using dynamic wormholes. One of the authors here has recently shown that for evolving (nonstatic) wormhole geometries it is possible to avoid the WEC violation of the required matter at least for a finite time interval [14].

However, the standard type of work done in other curved spacetimes, such as the study of geodesic motion, scalar waves, spin-half perturbations, electromagnetic, and gravitational perturbations, has not yet been dealt with completely in the context of wormholes. The papers which discuss scalar waves in wormhole geometries and in time-machine models are the ones referred to in Refs. [15, 10]. Very general statements regarding the well definedness of the Cauchy problem in a class of spacetimes with closed timelike curves (constructed from static wormholes) have been made by Friedmann and Morris [10]. Our aim, however, is to study the propagation of scalar waves through a static wormhole with a certain specific metric and without any closed timelike curves. The background spacetime is chosen as the simplest possible wormhole, first discussed extensively by Ellis [16] and later by Morris and Thorne [1]. We deal with both the (2+1)- and the (3+1)-dimensional versions of the metric. The scalar wave equation (massless) is written down and separated. It turns out that the radial equation (for the coordinate l) is a modified Mathieu equation in 2+1 dimensions. In 3+1 dimensions it is the radial equation that appears when the Helmholtz equation is separated in oblate spheroidal coordinates Both equations can be solved exactly. We discuss their solutions in detail and thereafter use them to understand the scattering of scalar waves in a wormhole geometry. The

*Electronic address: kars@iitk.ernet.in
†Electronic address: ds@iitk.ernet.in
‡Present address: IUCAA, Post Bag 4, Ganeshkind, Pune 411 007, India. Electronic address: biplab@iucaa.ernet.in

reflection and transmission coefficients are evaluated for both the (2+1)- and (3+1)-dimensional cases, for certain specific values of the energy of the scalar wave. We also comment on the possible differences that arise for the case of a massive scalar wave.

The paper is organized as follows. Section II discusses the wormhole metric and general features of wormholes in some detail. Section III deals with the scalar wave equation, the separation of variables, and the corresponding equivalent Schrödinger-type equations. In Sec. IV we discuss the solutions for both the 2+1 and 3+1 cases. The scattering problem is analyzed in Sec. V. Finally, Sec. VI is a conclusion with comments on certain unsolved issues.

II. THE WORMHOLE GEOMETRY

Spherically symmetric static Lorentzian wormholes are generically represented by the following form of the metric:

$$ds^2=-e^{2\Phi(r)}dt^2+\frac{dr^2}{1-b(r)/r}+r^2d\Omega^2 , \tag{1}$$

where $\Phi(r)$ is known as the redshift function, $b(r)$ the wormhole shape function, and $d\Omega^2\equiv d\theta^2$ (2+1 dimensions), $d\Omega^2=d\theta^2+\sin^2\theta\, d\phi^2$ (3+1 dimensions). The metric in (1) can be written alternatively by introducing the proper radial distance function $l(r)$ defined as

$$l(r)=\pm\int_{b_0}^{r}\frac{dr}{[1-b(r)/r]^{1/2}} . \tag{2}$$

This leads to the equivalent form of (1) given by

$$ds^2=-e^{2\kappa(l)}dt^2+dl^2+r^2(l)d\Omega^2 , \tag{3}$$

where $\kappa(l)$ is the functional form of $\phi(r)$ in the l coordinate and $r(l)$ is the inverse of $l(r)$. Notice that the variable l extends from $-\infty$ to $+\infty$ as r varies from 0 to ∞. For the metric to be a wormhole $b(r)$ and $\Phi(r)$ have to satisfy the conditions (i) $b(r)/r\le 1$, $b(r=b_0)=b_0$, (ii) $r\to\infty$, $b(r)/r\to 0$, and (iii) $\Phi(r)$ finite everywhere. In the l coordinate representation (i) and (ii) translate into (i) $l\to\pm\infty$, $r^2(l)\propto l^2$, and (ii) $l\to 0$, $r(l)\to b_0$. The condition on $\Phi(r)$ becomes an exactly identical condition on $\kappa(l)$. The simplest such wormhole metric is the one for which $\Phi=0$, $b(r)=b_0^2/r$ or $\kappa=0$, $r(l)=(b_0^2+l^2)^{1/2}$. One can show that when a $t=$const $\theta=\pi/2$ slice of the (3+1)-dimensional metric or a $t=$const slice of the (2+1)-dimensional analogue is embedded in flat R^3 the embedding function $z(r)$ is given by

$$z(r)=b_0\,\mathrm{arccosh}(r/b_0) . \tag{4}$$

It can also be shown that the Einstein equations of general relativity imply that such a metric can exist only if the classical energy-momentum tensor in the static observer's frame has a negative energy density. This is the background metric we shall use for studying scalar waves. We explicitly write out the metrics for the (2+1)- and (3+1)-dimensional cases below (in the l coordinate representation):

$$ds^2=-dt^2+dl^2+(b_0^2+l^2)d\theta^2 \qquad (2+1 \text{ dimensions}) , \tag{5}$$

$$ds^2=-dt^2+dl^2+(b_0^2+l^2)(d\theta^2+\sin^2\theta\, d\phi^2) \qquad (3+1 \text{ dimensions}) . \tag{6}$$

In the above $l\to+\infty$ and $\to-\infty$ correspond to the upper and lower asymptotically flat regions. $l=0$ is the throat region. We now write down the scalar wave equations for the two cases, separate them and solve them.

III. MASSLESS SCALAR WAVE EQUATION, SEPARATION OF VARIABLES, EQUIVALENT ONE-DIMENSIONAL PROBLEMS

The massless scalar wave equation is given by

$$g^{\mu\nu}\nabla_\mu\nabla_\nu\Phi=0 , \tag{7}$$

where ∇_μ denotes the covariant derivative. We shall discuss the (2+1)- and (3+1)-dimensional cases separately.

A. 2+1 dimensions

Using standard methods of separation of variables we find that the equations for the t, l, and θ coordinates reduce to the following. We assume

$$\Phi(t,l,\theta)=T(t)L(t)\Theta(\theta) . \tag{8}$$

Then,

$$\frac{d^2\Theta}{d\theta^2}+m^2\Theta=0 , \tag{9}$$

$$\frac{d^2T}{dt^2}+\omega^2T=0 , \tag{10}$$

$$(b_0^2+l^2)\frac{d^2L}{dl^2}+l\frac{dL}{dl}+[\omega^2(b_0^2+l^2)-m^2]L=0 . \tag{11}$$

The first two of these equations are simple. The third equation can be reduced to the following alternative forms. If we define a function $g(l)$ such that

$$L(l)=\frac{g(l)}{(b_0^2+l^2)^{1/4}} , \tag{12}$$

then (11) reduces to

$$\frac{d^2g}{dl^2}+\left[\omega^2-\left[\frac{2b_0^2-l^2}{4(b_0^2+l^2)^2}+\frac{m^2}{b_0^2+l^2}\right]\right]g=0 . \tag{13}$$

This is the equivalent one-dimensional problem (Schrödinger equation) with the role of energy being played by ω^2 and the potential function is given by the term in large parentheses. The allowed values of m are discrete in order that $\Theta(\theta)$ be single valued. The effective potential is plotted for various values of m in Fig. 1. For $m=0$ there are two minima situated at $l^2=5b_0^2$ and a maximum at $l=0$. If $m>0$ the potential has only a maximum at $l=0$. Asymptotically ($l\to\pm\infty$) the potential drops to a zero value. On the other hand, if one uses the transformation

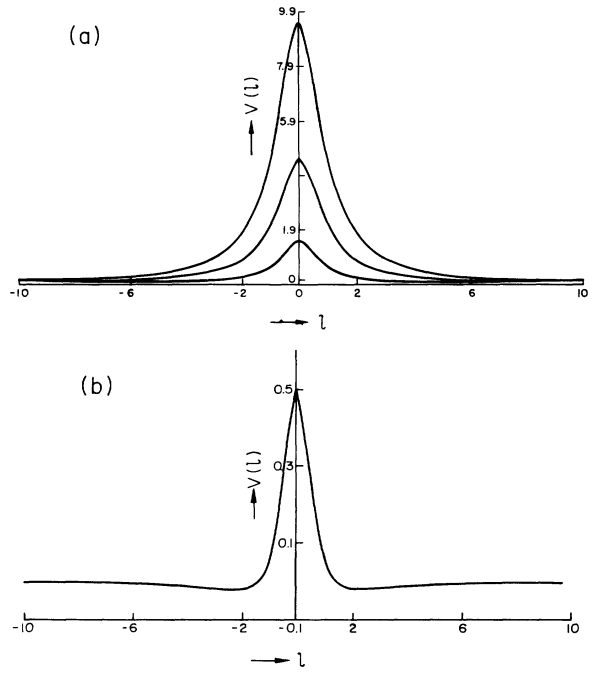

FIG. 1. (a) The $V(l)$ versus l plot for the effective potential in Eq. (13). b_0 is chosen as 1 and $m=1,2,3$ for the three curves with successively increasing values of the barrier at $l=0$. (b) The $v(l)$ versus l plot for the effective potential in Eq. (13). $b_0=1$ and $m=0$.

$$l=b_0\sinh\xi\ , \tag{14}$$

one can reduce (11) to the equation

$$\frac{d^2}{d\xi^2}L(\xi)-(a-2q\cosh 2\xi)L(\xi)=0\ , \tag{15}$$

where $a=m^2-\omega^2b_0^2/2$ and $q=\omega^2b_0^2/4$. The equation in (15) is known as the modified Mathieu equation with $a+2q=m^2$ as a constraint on the values of (a,q).

B. 3+1 dimensions

In 3+1 dimensions one can similarly use

$$\Phi(t,l,\theta,\phi)=T(t)L(l)\Theta(\theta)P(\phi)\ . \tag{16}$$

The corresponding equations for $T(t)$, $L(l)$, $\Theta(\theta)$, and $P(\phi)$ turn out to be

$$\frac{d^2T}{dt^2}+\omega^2T=0\ , \tag{17}$$

$$(b_0^2+l^2)\frac{d^2L}{dl^2}+2l\frac{dL}{dl}+[\omega^2(b_0^2+l^2)-p(p+1)]L=0\ , \tag{18}$$

$$\frac{1}{\sin\theta}\frac{d}{d\theta}\left[\sin\theta\frac{d\Theta}{d\theta}\right]+\left[p(p+1)-\frac{m^2}{\sin^2\theta}\right]\Theta=0\ , \tag{19}$$

$$\frac{d^2P}{d\phi^2}+m^2P=0\ . \tag{20}$$

The solutions to (19) and (20) comprise the spherical harmonics. As in the 2+1-dimensional case Eq. (18) can also be reduced to an equivalent Schrödinger-type equation of the form

$$\frac{d^2F}{dl^2}+\left[\omega^2-\left[\frac{b_0^2}{(b_0^2+l^2)^2}+\frac{p(p+1)}{(b_0^2+l^2)}\right]\right]F=0\ , \tag{21}$$

where we have

$$L(l)=\frac{F(l)}{(b_0^2+l^2)^{1/2}}\ . \tag{22}$$

On the other hand, by introducing $\xi=l/b_0$ we can write (18) in the form

$$(1+\xi^2)\frac{d^2L}{d\xi^2}+2\xi\frac{dL}{d\xi}+[\omega^2b_0^2(1+\xi^2)-p(p+1)]L=0\ . \tag{23}$$

The Helmholtz equation $(\nabla^2+k^2)\psi=0$ when separated in oblate spheroidal coordinates (see Appendix) yields a radial equation of the form

$$(1+\xi^2)\frac{d^2v_{mn}}{d\xi^2}+2\xi\frac{dv_{mn}}{d\xi}+\left[-\lambda_{mn}+k^2\xi^2-\frac{m^2}{1+\xi^2}\right]v_{mn}=0\ . \tag{24}$$

For $m=0$ this equation is exactly the same as (23) with the identifications

$$\lambda_{0n}=p(p+1)-\omega^2b_0^2 \quad\text{and}\quad k^2=\omega^2b_0^2\ . \tag{25}$$

Therefore, $\lambda_{0n}+k^2=p(p+1)$ is a constraint on the allowed values of λ_{0n}, which are essentially functions of k^2.

The potential function in (21) is plotted in Fig. 2. For all l this is a barrier-type potential with the barrier situated at $l=0$. We have, therefore, reduced the study of scalar waves to a one-dimensional scattering problem in traditional quantum mechanics. The reflection and transmission coefficients across the barrier can now be evaluated very easily. However, before we do that it is essential to understand certain important characteristic features of the functions which are the solutions of (15) and (23). This is dealt with in the subsequent section.

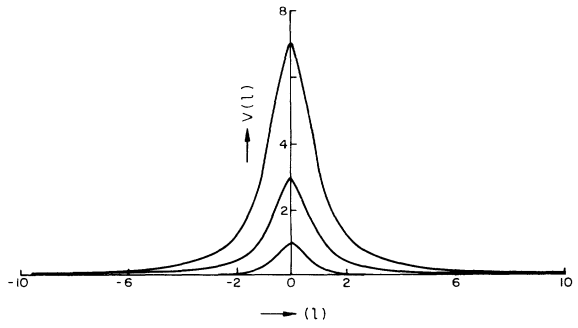

FIG. 2. The $V(l)$ versus l plot for the effective potential in Eq. (21). b_0 is chosen as (1) and $p=0,1,2$ for the three curves with successively increasing values of the barrier at $l=0$.

IV. THE EXACT SOLUTIONS IN 2+1 AND 3+1 DIMENSIONS

The full solution of the wave equation in 2+1 dimensions will be (see Appendix)

$$\Phi(t,l,\theta)\approx e^{\pm i\omega t}e^{\pm im\theta}\times\begin{cases} AMc^{(1)}_{2n,2n+1}+BMc^{(2)}_{2n,2n+1} & \text{for } a_{2n}\ , \\ CMs^{(1)}_{2n,2n+1}+DMs^{(2)}_{2n,2n+1} & \text{for } b_{2n}\ , \end{cases} \tag{26}$$

where $Mc^{(1)}_{2n,2n+1}$ and $Mc^{(2)}_{2n,2n+1}$ are a fundamental system for the l coordinate equations for the characteristic values a_{2n} and a_{2n+1}. $Ms^{(1)}_{2n,2n+1}$ and $Ms^{(2)}_{2n,2n+1}$ form the fundamental system for which the characteristic values are b_{2n} and b_{2n+1}. Known solutions to the modified Mathieu equation are essentially of two types—integral order and fractional order. In the above we have written down the solutions for integral order only. Thus we have chosen specific values of (a,q) that lie on the characteristic lines. These values are the ones we get when we intersect the characteristic lines with the straight lines $a+2q=m^2$. Other values of (a,q) which lie on the lines $a+2q=m^2$ and fall in the regions between the curves a_i and b_{i+1} give rise to the fractional order modified Mathieu functions. It is worthwhile to note that for $m=0$ there are known solutions for positive values of q. The diagram shown in Fig. 3 demonstrates the facts discussed above. Details about the modified Mathieu functions can be found in the Appendix of this paper. It is necessary to realize that all the information regarding the reflection and transmission of scalar waves can be obtained by properly analyzing the solutions of the l coordinate differential equation. The asymptotic forms of the various solutions are essential ingredients for understanding scattering phenomena. Below we discuss the asymptotic forms of $Mc^{(1)}$ and $Mc^{(2)}$ as $l\to+\infty$ and $\to-\infty$ in some detail. We shall work with the solutions on the characteristic lines a_{2n}, thus considering only $Mc^{(1)}_{2n}$ and $Mc^{(2)}_{2n}$. For all other cases the analysis is very similar.

Using the Bessel function series representations for the functions $Mc^{(1)}_{2n}$ and $Mc^{(2)}_{2n}$ we first analyze the limit $l\to\infty$ ($\xi\to\infty$). The series for $Mc^{(1)}_{2n}$ is valid for all ξ ($-\infty<\xi<\infty$) whereas for $Mc^{(2)}_{2n}$ it is valid only for $\xi>0$. Moreover, $Mc^{(1)}_{2n}$ is an even function whereas $Mc^{(2)}_{2n}$ is neither even nor odd.

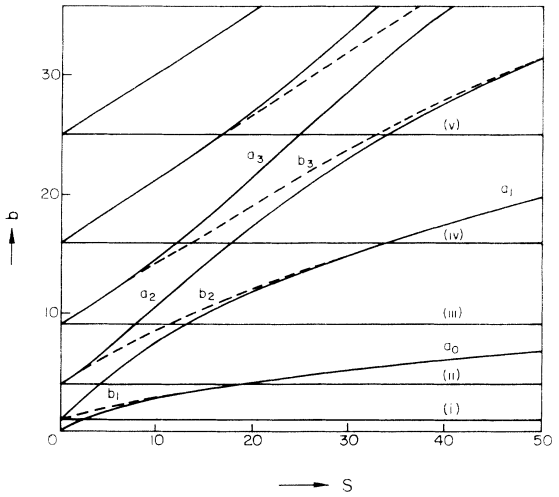

FIG. 3. The b versus S plot for the characteristic lines. Here $b=m^2$ and $S=\omega^2 b_0^2$. In relation to a,q we have $S=4q$ and $a+2q=b$. The regions between the a_i and b_{i+1} curves are the "stability regions." (i), (ii), (iii), (iv), and (v) correspond to $m=1$, 2, 3, 4, and 5, respectively (i.e., $b=1$, 4, 9, 16, and 25).

A. Asymptotic forms for $\xi\to\infty$ ($l\to\infty$)

The asymptotic forms for $\xi\to\infty$ ($l\to\infty$) are the following:

$$Mc^{(1)}_{2n}\to\left[[ce_{2n}(0,q)]^{-1}\sum_{k=0}^{\infty}(-1)^n A^{2n}_{2k}(q)\right]\times\left[\frac{1}{\pi\sqrt{q}\cosh\xi}\right]^{1/2}\cos(2\sqrt{q}\cosh\xi-\pi/4)\ , \tag{27}$$

$$Mc^{(2)}_{2n}\to\left[[ce_{2n}(0,q)]^{-1}\sum_{k=0}^{\infty}(-1)^n A^{2n}_{2k}(q)\right]\times\left[\frac{1}{\pi\sqrt{q}\cosh\xi}\right]^{1/2}\sin(2\sqrt{q}\cosh\xi-\pi/4)\ . \tag{28}$$

B. Asymptotic forms for $\xi\to-\infty$ ($l\to-\infty$)

The arguments for analytically extending $Mc^{(1)}_{2n}$ for $\xi<0$ are presented in the Appendix. Here we just state the result:

$$Mc^{(1)}_{2n}\to\left[[ce_{2n}(0,q)]^{-1}\sum_{k=0}^{\infty}(-1)^n A^{2n}_{2k}(q)\right]\left[\frac{1}{\pi\sqrt{q}\cosh\xi}\right]^{1/2}\cos(2\sqrt{q}\cosh\xi-\pi/4)\ , \tag{29}$$

$$Mc^{(2)}_{2n}\to\left[[ce_{2n}(0,q)]^{-1}\sum_{k=0}^{\infty}(-1)^n(q)\left[\frac{1}{\pi\sqrt{q}\cosh\xi}\right]^{1/2}\right][-\sin(2\sqrt{q}\cosh\xi-\pi/4)-2f_{e,2n}\cos(2\sqrt{q}\cosh\xi-\pi/4)]\ , \tag{30}$$

where ce_{2n} is the ordinary Mathieu function evaluated at $\xi=0$ and

$$f_{e,2n}=-\frac{Mc_{2n}^{(2)}(0,q)}{Mc_{2n}^{(1)}(0,q)} . \tag{31}$$

$f_{e,2n}$ are known as the joining factors and are tabulated in Refs. [17, 18].

A remark about the allowed values of (a,q) or $\omega^2 b_0^2$ is in order now. We note that solutions to the l equations are possible only for certain ranges (bands) of energies of the scalar wave. The edges of the bands lie on the characteristic curves and therefore correspond to integral order solutions. The region within the curves a_i and b_{i+1} lying on $a+2q=m^2$ but excluding the end points corresponds to fractional order modified Mathieu functions $Ce_{2n+\beta}$ and $Se_{2n+\beta}$, which can coexist for a values $a_{2n+\beta}$. However, while discussing the scattering of scalar waves we shall consider only those values of the energy which lie on the characteristic lines. In other words, we deal with only the integral order modified Mathieu functions.

In $3+1$ dimensions the situation is quite similar to the $(2+1)$-dimensional case. The full solution to the scalar wave equation is now of the form

$$\Phi(t,l,\theta,\varphi)\approx e^{\pm i\omega t}e^{\pm im\phi}P_{\phi}^{|m|}(\cos\theta) \times \begin{cases} Av_{n0}^{(1)}(\xi)+Bv_{n0}^{(2)}(\xi) & n \text{ even} , \\ Cv_{n0}^{(1)}(\xi)+Dv_{n0}^{(2)}(\xi) & n \text{ odd} . \end{cases} \tag{32}$$

We have written two different sets of solutions for n odd and n even with the same notation $v_{n0}^{(1)}$, $v_{n0}^{(2)}$. It should be noted that the functional series representations for n odd and n even are not entirely identical. In this case also we have a constraint on the allowed values of λ_{0n} [this is the condition $\lambda_{0n}=-k^2+p(p+1)$]. Therefore, we have to draw the lines $\lambda_{0n}=-k^2+p(p+1)$ on the λ_{0n}-k^2 plot for the characteristic curves. Each value of p gives a certain straight line which cuts the $n=0,1,\ldots$ curves at specific points. These points denote the specific values of k^2 for which we have the solutions $v_{0n}^{(1)}$ and $v_{0n}^{(2)}$.

The asymptotic forms for $v_{0n}^{(1)}$ and $v_{0n}^{(2)}$ can be written down from Ref. [16]. These are as follows. For $\xi\to-\infty$ we use the fact that $v_{0n}^{(2)}$ is neither even nor odd and define joining factors by which we analytically extend the solutions to the $\xi<0$ region:

$\xi\to+\infty$:

$$v_{n0}^{(1)}(\xi)\to\frac{q_{n0}}{k\xi}\sin k\xi, \quad n \text{ even} , \tag{33}$$

$$v_{n0}^{(1)}(\xi)\to-\frac{iq_{n0}}{k\xi}\sin k\xi, \quad n \text{ odd} , \tag{34}$$

$$v_{n0}^{(2)}(\xi)\to-\frac{q_{n0}}{k\xi}\cos k\xi, \quad n \text{ even} , \tag{35}$$

$$v_{n0}^{(2)}(\xi)\to-\frac{iq_{n0}}{k\xi}\sin k\xi, \quad n \text{ odd} , \tag{36}$$

$\xi\to-\infty$:

$$v_{n0}^{(1)}(\xi)\to\frac{q_{n0}}{k\xi}\sin k\xi, \quad n \text{ even} , \tag{37}$$

$$v_{n0}^{(1)}(\xi)\to-\frac{iq_{n0}}{k\xi}\cos k\xi, \quad n \text{ odd} , \tag{38}$$

$$v_{n0}^{(2)}(\xi)\to-\frac{q_{n0}}{k\xi}\cos k\xi-2h_{e,n}\frac{q_{n0}}{k\xi}\sin k\xi, \quad n \text{ even} , \tag{39}$$

$$v_{n0}^{(2)}(\xi)\to-\frac{iq_{n0}}{k\xi}\sin k\xi-2ic_{e,n}\frac{q_{n0}}{k\xi}\cos k\xi, \quad n \text{ odd} , \tag{40}$$

where

$$h_{e,n}=-\frac{v_{n0}^{(2)}(0)}{v_{n0}^{(1)}(0)}, \quad c_{e,n}=\frac{v_{n0}^{(2)\prime}(0)}{v_{n0}^{(1)\prime}(0)} , \tag{41}$$

and q_{n0} are constants while the exact form (see Ref. [1]) is irrelevant for our purpose.

We now have all the essential material to study the scattering problem in both $2+1$ and $3+1$ dimensions. It will be shown that the reflection and transmission coefficients depend on the "joining factors" for each of the cases. In $3+1$ dimensions, we are unaware of the existence of fractional order solutions, stability zones, and associated characteristics similar to the $(2+1)$-dimensional case. Also the "joining factors" for $3+1$ dimensions are not tabulated as they are for $2+1$ dimensions.

V. SCATTERING, REFLECTION, AND TRANSMISSION COEFFICIENTS

In order to deal with the scattering of scalar waves it is necessary to go back to the equivalent one dimensional Schrödinger equations derived from the original l coordinate equation in Sec. III. The relationship between the functions $L(l)$ and $g(l)$ is given in (12). We know the solution $L(\xi)$ which can be written in terms of l using the inverse relationship $\xi=\operatorname{arcsinh}(l/b_0)$. The two linearly independent solutions to the Schrödinger equations are therefore given as

$$g^{(i)}(l)=(b^2+l^2)^{1/4}Mc_{2n}^{(i)}(\xi,q) , \tag{42}$$

where i takes the values 1 and 2. In the previous section we had discussed the asymptotic forms of $Mc_{2n}^{(i)}$ in detail. The corresponding asymptotic forms for $g^{(i)}(l)$ are therefore given by

$l\to+\infty$:

$$g^{(1)}(l)=\left[\frac{2}{\pi\omega}\right]^{1/2}A_1\cos(\omega l-\pi/4) , \tag{43}$$

$$g^{(2)}(l)=\left[\frac{2}{\pi\omega}\right]^{1/2}A_1\sin(\omega l-\pi/4) , \tag{44}$$

$l \to -\infty$:

$$g^{(1)}(l) = \left[\frac{2}{\pi\omega}\right]^{1/2} A_1 \cos(\omega l - \pi/4) , \tag{45}$$

$$g^{(2)}(l) = \left[\frac{2}{\pi\omega}\right]^{1/2} A_1 [-\sin(\omega l - \pi/4) - 2 f_{e,2n} \cos(\omega l - \pi/4)] , \tag{46}$$

where

$$A_1 = [ce_{2n}(0,q)]^{-1}(-1)^n \sum_{k=0}^{\infty} A_{2k}^{2n}(q) .$$

Now, as $l \to \infty$ we want only a right-moving transmitted wave. The linear combination of interest is therefore given by

$$\lim_{l\to\infty} [g^{(1)}(l) + i g^{(2)}(l)] = \bar{A}_1 e^{-i\pi/4} e^{i\omega l} , \tag{47}$$

where we now have set

$$\bar{A}_1 = A_1 (2/\pi\omega)^{1/2} .$$

At $l \to -\infty$ we have an incident wave and a reflected wave. Thus,

$$\lim_{l\to-\infty} \bar{A}_1 [-i f_{e,2n} e^{-i\pi/4} e^{-i\omega l} + (1 - i f_{e,2n}) e^{i\pi/4} e^{i\omega l}] . \tag{48}$$

Hence the reflection and transmission coefficients are given by

$$R = \frac{-f_{e,2n}}{1 - i f_{e,2n}}, \quad T = \frac{-i}{1 - i f_{e,2n}} . \tag{49}$$

It is easy to see from (49) that

$$|R|^2 + |T|^2 = 1 . \tag{50}$$

A similar analysis can be done for the $(Mc_{2n+1}^{(1)}, Mc_{2n+1}^{(2)})$ and the $(Ms^{(1)}, Ms^{(2)})$ functions. Thus for certain specific values of the energies obtained by intersecting the characteristic curves with the lines $a + 2q = m^2$ we have the R and T given by (49). Using the tables given in Refs. [17, 18] we can now evaluate the R and T for those values explicitly. A short table of values is given in Table I. The values of $|R|$ there suggest that both "near-perfect" reflection as well as transmission are possible.

In 3+1 dimensions the solution of the scattering problem is similar. We shall only be dealing with the case for which n is even. The relationship between $L(\xi)$ and $F(\xi)$ is given in (22). The asymptotic forms for $F_n^{(1)}(\xi)$ and $F_n^{(2)}(\xi)$ as $\xi \to \pm\infty$ are given below:

$\xi \to \infty$:

$$F_n^{(1)}(\xi) \to \frac{q_{n0}}{k} \sin k\xi , \qquad F_n^{(2)}(\xi) \to -\frac{q_{n0}}{k} \cos k\xi . \tag{51}$$

The linear combination at $\xi \to \infty$ which gives us a purely right-moving transmitted wave is $F_n^{(1)}(\xi) + i F_n^{(2)}(\xi)$.

TABLE I. Reflection coefficients for various values of S_m and m. S_m refers to the points of intersection of the line $b = m^2$ with the characteristic curves. $f_{e,r}$ is the joining factor for $Mc_r^{(2)}$ and $f_{0,r}$ the same for $Ms_r^{(2)}$. $|R|$ denotes the absolute value of the reflection coefficient of a "circular" wave with certain value of m and ωb_0 (5).

m	S_m	$f_{e,r}, f_{0,r}$	$\lvert R\rvert$
1	2.25 (a_0)	0.2867	0.2755
2	4.25 (a_1)	0.9280	0.6802
	18.5 (a_0, b_1)	0.0025	0.0025
3	7.75 (a_2)	2.099	0.9028
	11.25 (b_2)	0.3610	0.3396
	13.25 (a_1)	0.1666	0.1644
4	12.00 (a_3)	5.8009	0.9854
	13.75 (b_3)	2.8064	0.9419
	18.00 (a_2)	0.5272	0.4663
	33.75 (a_1, b_2)	0.0059	0.0059
5	16.75 (a_4)	21.482	0.9989
	17.00 (b_4)	18.7585	0.9986
	25.00 (a_3)	1.1046	0.7413
	33.00 (b_3)	0.1129	0.1122
	34.25 (a_2)	0.0835	0.0832

Indeed

$$\lim_{\xi\to+\infty} [F_n^{(1)}(\xi) + i F_n^{(2)}(\xi)] \to \frac{-i q_{n0}}{k} e^{ik\xi} , \tag{52}$$

where q_{n0} are constants given in Ref. [19].

As in the 2+1-dimensional case, for $\xi \to -\infty$ we will have the joining factors coming into the picture. Therefore,

$$\lim_{\xi\to-\infty} \frac{i q_{n0}}{k} [(1 - i h_{e,n}) e^{ik\xi} + i h_{e,n} e^{-ik\xi}] . \tag{53}$$

The reflection and transmission coefficients turn out to be

$$R = \frac{+i h_{e,n}}{1 - i h_{e,n}}, \quad T = \frac{-1}{1 - i h_{e,n}} . \tag{54}$$

Once again it is clear from (53) that $|R|^2 + |T|^2 = 1$.

VI. DISCUSSIONS AND CONCLUSIONS

We may summarize the results of the paper as follows.

(i) The primary motivation of this paper has been to use scalar waves as a method of studying the properties of the wormhole. To this end we have exactly solved the massless Klein-Gordon equation in a wormhole background both in 2+1 and 3+1 dimensions. The plots of the effective potentials in Figs. 1 and 2 have shown us that these are barrier-type potentials. Hence we have studied the "reflection" and "transmission" of incident "circular" and "spherical" waves. In 2+1 dimensions, the properties of the solutions of the modified Mathieu equation has enabled us to evaluate the "reflection coefficient" for specific values of the quantity ωb_0. In fact, we have also seen that unless ωb_0 lies within certain ranges and satisfies $a + 2q = m^2$ we are unable to write down explicit solutions. For this specific range of values of ωb_0 the scattering of scalar waves can be understood using the known solutions to the wave equation (which

are finite at infinity). The values of $|R|$ given in Table I confirm the physically obvious fact that for higher values of ω (b_0 fixed) the reflection is less whereas there is more transmission. The opposite happens for lower values of ω. If ωb_0 is outside the regions between a_i and b_{i+1} explicit solutions are not known and we are unable to analyze the problem. A similar situation also exists in 3+1 dimensions.

It is important to note the differences between our analysis and the one due to Clement [15]. Clement's basic motivation was to demonstrate the fact that the "wormhole geometry" is a "particlelike" object. In order to do that he used the scattering of scalar and electromagnetic waves as probes. By analyzing the "phase shifts" due to the scattering of incident phase waves he arrived at certain interesting conclusions supporting the conjecture that "wormholes" are, in fact, like "particles." His work is essentially an important one in the context of the Wheeler-Misner concept of visualizing classical physics as manifest in just the geometry of spacetime. As mentioned in the introductory sections of this paper the context in which "wormholes" are discussed in recent times is somewhat different.

(ii) One can also visualize the reflection and transmission of scalar waves in the following alternative way. The wormhole has two asymptotic regions ($l\to\infty$, $l\to-\infty$). Suppose we have an observer in the $l\to-\infty$ region. He sees a certain wave being sent in through the throat. As he is totally unaware of the existence of another asymptotic region he can think that the incident wave is, in a sense, partially "absorbed" and partially reflected. In fact, he can, in principle, use his intellectual abilities to predict that he is in a wormhole geometry and not just in flat space. The existence of a "tunnel" to the "other universe" is a primary cause of certain characteristic properties of the reflection and transmission of scalar waves of specific values of m and p (as well as ωb_0) in 2+1 and 3+1 dimensions, respectively.

(iii) The obvious question that one can ask is "What happens if we send in a massive scalar wave?" The answer to this is almost trivial. If one response is ω^2 by $\omega^2+m^2=\omega'^2$ one can repeat the same analysis as for the massless case without any modifications. The parameters a and q will have their values in terms of ω'^2. Hence the possible values of ωb_0 will change when viewed relative to the massless case. In 3+1 dimensions also a similar situation arises. The complete study of "perturbation" of a wormhole geometry would actually require understanding the "reflection" and "transmission" of "electromagnetic waves" as well as "spin-half" waves (the Dirac equations) as well as the problem of general gravitational perturbations. Work along these lines is in progress and will be communicated in the future.

(iv) Finally, we mention the following analogy. The fact that the geometry used in this paper has a "catenoidal" spacelike section when embedded in $\mathbb{R}^3$ implies that it is a "minimal surface" (a surface of zero mean curvature). Such surfaces occur when one studies soap films formed between rings. Thus, our study of scalar waves is in principle a study of the vibrational modes of the soap film modulo the fact that appropriate boundary conditions have to be employed for the latter. Using exactly the same analysis (2+1 case) one can actually comment on the stability of such films. A detailed understanding of this analogous problem will be dealt with separately later.

ACKNOWLEDGMENTS

The authors thank Shiraz Minwalla and Deepak Mishra for helpful discussions. S.K. thanks the Department of Science and Technology, Government of India for financial support.

APPENDIX: MODIFIED MATHIEU FUNCTIONS AND RADIAL OBLATE SPHEROIDAL WAVE FUNCTIONS

1. Modified Mathieu functions

Several authors have discussed Mathieu and modified Mathieu functions in great detail [17, 18, 20, 21]. In this appendix we collect some of the relevant material, in order to make this paper self-contained.

The original Mathieu equation which Mathieu had studied is of the form

$$\frac{d^2y}{dz^2}+(a-2q\cos 2z)y=0\ . \tag{A1}$$

Replacing z by iz we arrive at the modified Mathieu equation

$$\frac{d^2y}{dz^2}-(a-2q\cosh 2z)y=0\ . \tag{A2}$$

We shall not go any further into discussing the solutions of (A1). Rather we shall concentrate on the solutions of (A2). It is worthwhile to mention that (A1) and (A2) appear when the Helmholtz equation $(\nabla^2+k^2)\psi=0$ is separated in elliptic-cylindrical coordinates.

Solutions to (A2) are dependent on the values of a and q (or b and s). In fact, the b-s plot shown in Fig. 3 demonstrates this fact clearly. The solid lines (marked a_0, a_1, b_1, etc.) on the plot are known as the characteristic lines. Values of (a,q) lying on these lines yield solutions to (A2) known as Mathieu functions of integral order. These are the functions $Mc^{(1)}_{2n}$, $Mc^{(1)}_{2n+1}$, $Ms^{(1)}_{2n}$, and $Ms^{(1)}_{2n+1}$ for a values lying on the a_{2n}, a_{2n+1}, b_{2n}, and b_{2n+1} curves, respectively. These functions can be represented by infinite series in various ways. The most common of these representations are the cosh or sinh series, the Bessel function series, and the one in terms of products of Bessel functions. The first one of these representations is given below:

$$Mc^{(1)}_{2n}=\frac{(-1)^n A^{2n}_0}{ce_{2n}(\pi/2,q)[ce_{2n}(0,q)]}\sum_{k=0}^{\infty}A^{2k}_{2n}(q)\cosh 2kz\ , \tag{A3a}$$

$$Mc^{(1)}_{2n+1}=\frac{(-1)^{n+1}A^{2n+1}_1\sqrt{q}}{ce'_{2n}(\pi/2,q)[ce_{2n+1}(0,q)]}\times\sum_{k=0}^{\infty}A^{2k+1}_{2n+1}(q)\cosh(2k+1)z\ , \tag{A3b}$$

$$Ms^{(1)}_{2n}=\frac{(-1)^{n}qB^{2n}_2}{se'_{2n}(0,q)Se'_{2n}(\pi/2,q)}\sum_{k=0}^{\infty}B^{2k}_{2n}(q)\sinh 2kz\ , \tag{A3c}$$

$$Ms^{(1)}_{2n+1}=\frac{(-1)^{n+1}B^{2n+1}_1\sqrt{q}}{se'_{2n+1}(0,q)se_{2n+1}(\pi/2,q)}\times\sum_{k=0}^{\infty}B^{2k+1}_{2n+1}(q)\sinh(2k+1)z\ . \tag{A3d}$$

The $Mc^{(1)}_{2n}$, $Mc^{(1)}_{2n+1}$, $Ms^{(1)}_{2n}$, and $Ms^{(1)}_{2n+1}$ form the "basically periodic" solutions of the Mathieu equation. $Mc^{(1)}_{2n}$ and $Ms^{(1)}_{2n}$ or any such pair cannot coexist for the same values of (a,q). Thus we require a second solution to the modified Mathieu equation. These second solutions are the $Mc^{(2)}$ and $Ms^{(2)}$ corresponding to $Mc^{(1)}$ and $Ms^{(1)}$, respectively. The $Mc^{(1)}$ and $Ms^{(1)}$ are even and odd solutions, respectively. A theorem due to Ince [18] says that the $Mc^{(2)}$ and $Ms^{(2)}$ are functions which are neither even nor odd. The Bessel function series representations are given below. The series involving the J Bessel functions are valid for all z. On the other hand, the series involving the Neumann (Y Bessel function) functions are valid for $z>0$. We shall discuss later in this Appendix how to analytically continue the $Mc^{(2)}$ or $Ms^{(2)}$ for $z<0$:

$$Mc^{(i)}_{2n}=[ce_{2n}(0,q)]^{-1}\sum_{k=0}^{\infty}(-1)^{k+n}A^{2n}_{2k}(q)\times Z^{(j)}_{2k}(2\sqrt{q}\cosh z)\ , \tag{A4}$$

$$Ms^{(i)}_{2n}=[se'_{2n}(0,q)]^{-1}\tanh z\sum_{k=1}^{\infty}(-1)^{k+n}2kB^{2n}_{2k}(q)\times Z^{(j)}_{2k}(2\sqrt{q}\cosh z)\ . \tag{A5}$$

The formulas for a_{2n+1} and b_{2n+1} are exactly identical with $2n\to 2n+1$ and $2k\to 2k+1$. $Z^{(j)}_{2k}$ denotes a J Bessel function for $j=1$ and a Y Bessel function of $J=2$.

We now move on to the analysis for $z<0$. This is based on Sec. 20.6.18 of Ref. [17]. Consider two combinations

$$X_1=Mc^{(2)}_r(z,q)+Mc^{(2)}_r(-z,q)\ , \tag{A6a}$$

$$X_2=Ms^{(2)}_r(z,q)-Ms^{(2)}_r(-z,q)\ . \tag{A6b}$$

X_1 is even and therefore proportional to $Mc^{(1)}_r(z,q)$. X_2 is odd and proportional to $Ms^{(1)}_r(z,q)$. The proportionality factors are evaluated by using the values of the functions at $z=0$. It turns out that

$$Mc^{(2)}_r(-z,q)=-Mc^{(2)}_r(z,q)-2f_{e,r}Mc^{(2)}_r(z,q)\ , \tag{A7a}$$

$$Ms^{(2)}_r(-z,q)=Ms^{(2)}_r(z,q)-2g_{e,r}Ms^{(2)}_r(z,q)\ , \tag{A7b}$$

where

$$f_{e,r}=-Mc^{(2)}_r(0,q)/Mc^{(1)}_r(0,q)\ ,$$

$$g_{e,r}=\left[\frac{d}{dz}Ms^{(2)}_r(z,q)\Big/\frac{d}{dz}Ms^{(1)}_r(z,q)\right]_{z=0}\ .$$

The asymptotic forms for the functions $Mc^{(1)}$, $Mc^{(2)}$, $Ms^{(1)}$, and $Ms^{(2)}$ have been discussed earlier, and therefore are not repeated here.

Apart from the integral order solutions the Mathieu equation as well as the modified Mathieu equation has a solution of real fractional order. The regions between a_i and b_{i+1} in the plot correspond to the region of stability. Within these regions and away from the characteristic lines we have these fractional order solutions. The functions $Ce_{2n+\beta}$ and $Se_{2n+\beta}$ are not basically periodic and can coexist for the same value of $a_{2n+\beta}$.

2. The radial oblate spheroidal functions

If we separate the Helmholtz equation in oblate spheroidal coordinates the radial equation has the form given in (24). However, we are concerned with only the $m=0$ case, i.e., the functions v_{0n}. Once again, as in the Mathieu case, we have a set of solutions which are even or odd according to whether n is even or odd. These are known as the first solutions and we denote them by $v^{(1)}_{0n}$. The second solutions are neither even nor odd and correspond to a second set $v^{(2)}_{0n}$. Both $v^{(1)}_{0n}$ and $v^{(2)}_{0n}$ exist for the values of λ_{0n} which lie on the characteristic lines shown in Fig. 4. The analytical continuation to values of $z<0$ is based on the same analysis as for the case of modified Mathieu functions. (Unfortunately we are not aware of the existence of tables for the joining factors in this case. Therefore, we have to remain satisfied with the analytical expressions only.)

It is useful to make the correspondence between the $v^{(1)}_{0n}$ and the $v^{(2)}_{0n}$ and the $Mc^{(1)}$, $Mc^{(2)}$, $Ms^{(1)}$, and $Ms^{(2)}$

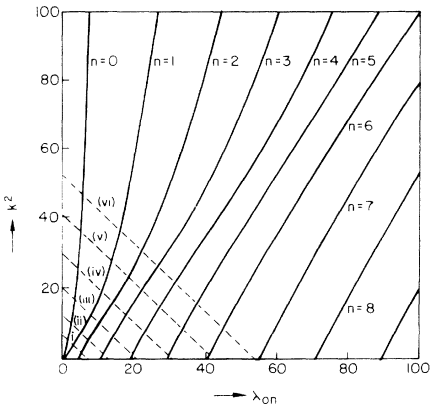

FIG. 4. The λ_{0n} versus k^2 plot for the characteristic lines for the oblate spheroidal wave functions with $m=0$. (i), (ii), (iii), (iv), and (v) refer to the straight lines $\lambda_{0n}=-k^2+p(p+1)$, where $p=2$, 3, 4, 5, 6, and 7, respectively.

clearer. $v_{0n}^{(1)}$ for n even is the analogue of $Mc^{(1)}$ and $v_{0n}^{(1)}$ for n odd is similar to $Ms^{(1)}$. $v_{0n}^{(2)}$ (n even) and $v_{0n}^{(2)}$ (n odd) correspond to $Mc^{(2)}$ and $Ms^{(2)}$, respectively. The series representations for the $v_{0n}^{(i)}$ ($i=1,2$) are given in Refs. [19, 22]. Leitner and Spence [19] have discussed the oblate spheroidal wave functions in great detail. The reader interested in spheroidal wave functions in general is referred to Refs. [22–25].

[1] M. S. Morris and K. S. Thorne, Am. J. Phys. **56**, 395 (1988).

[2] M. S. Morris, K. S. Thorne, and U. Yurtsever, Phys. Rev. Lett. **61**, 1446 (1988).

[3] H. Epstein, V. Glaser, and A. Jaffe, Nuovo Cimento **36**, 2296 (1965).

[4] H. B. G. Casimir, Proc. K. Ned. Akad. Wet. **51**, 793 (1948).

[5] D. Hochberg and T. W. Kephart, Phys. Lett. B **268**, 377 (1991).

[6] D. Hochberg, Phys. Lett. B **251**, 349 (1990).

[7] J. W. Moffat and T. Svobada, Phys. Rev. D **44**, 429 (1991).

[8] B. Bhawal and S. Kar, Phys. Rev. D **46**, 2464 (1992).

[9] M. Visser, Phys. Rev. D **39**, 3182 (1989); Nucl. Phys. **B328**, 203 (1989).

[10] J. Friedman, M. S. Morris, I. D. Novikov, F. Echeverria, G. Klinkhammer, K. S. Thorne, and U. Yurtsever, Phys. Rev. D **42**, 1915 (1990); J. Friedman and M. S. Morris, Phys. Rev. Lett. **66**, 401 (1991).

[11] S. Y. Kim, Phys. Rev. D **46**, 2428 (1992).

[12] T. A. Roman, Phys. Rev. D **47**, 1370 (1993).

[13] D. Hochberg and T. W. Kephart, Phys. Rev. Lett. **70**, 2665 (1993).

[14] Sayan Kar, Phys. Rev. D **49**, 862 (1994).

[15] G. Clement, Int. J. Theor. Phys. **23**, 335 (1984).

[16] H. Ellis, J. Math. Phys. **14**, 104 (1973).

[17] *Handbook of Mathematical Functions with Formulas, Graphs and Mathematical Tables,* edited by M. Abramowitz and I. A. Stegun (Dover, New York, 1965).

[18] *National Bureau of Standards, Tables Relating to Mathieu Functions* (Columbia University Press, New York, 1951).

[19] A. Leitner and R. D. Spence, J. Franklin Inst. **249**, 229 (1950).

[20] F. M. Arscott, *Periodic Differential Equations* (Macmillan, New York, 1964).

[21] N. W. MacLachlan, *Theory and Applications of Mathieu Functions* (Dover, New York, 1964).

[22] C. Flammer, *Spheroidal Wave Functions* (Stanford University Press, Stanford, CA, 1957).

[23] J. A. Stratton, P. M. Morse, L. J. Chu, and R. A. Hutner, *Elliptic Cylinder and Spheroidal Wave Functions* (Wiley, New York, 1941).

[24] P. M. Morse and H. Feshbach, *Methods of Theoretical Physics* (McGraw-Hill, New York, 1953).

[25] *Higher Transcendental Functions* (Bateman Manuscript Project), edited by A. Erdelyi *et al.* (McGraw-Hill, New York, 1953), Vol. 3.